Precipitation scaling with temperature in warm and cold climates: an analysis of CMIP5 simulations

Precipitation scaling with temperature in warm and cold climates: An analysis of CMIP5 simulations

Guangqi Li,[1] Sandy P. Harrison,[1,2] Patrick J. Bartlein,[3] Kenji Izumi,[3] and I. Colin Prentice[1,4]

Received 10 May 2013; revised 3 July 2013; accepted 9 July 2013; published 2 August 2013.

[1] We investigate the scaling between precipitation and temperature changes in warm and cold climates using six models that have simulated the response to both increased CO_2 and Last Glacial Maximum (LGM) boundary conditions. Globally, precipitation increases in warm climates and decreases in cold climates by between 1.5%/°C and 3%/°C. Precipitation sensitivity to temperature changes is lower over the land than over the ocean and lower over the tropical land than over the extratropical land, reflecting the constraint of water availability. The wet tropics get wetter in warm climates and drier in cold climates, but the changes in dry areas differ among models. Seasonal changes of tropical precipitation in a warmer world also reflect this "rich get richer" syndrome. Precipitation seasonality is decreased in the cold-climate state. The simulated changes in precipitation per degree temperature change are comparable to the observed changes in both the historical period and the LGM. **Citation:** Li, G., S. P. Harrison, P. J. Bartlein, K. Izumi, and I. Colin Prentice (2013), Precipitation scaling with temperature in warm and cold climates: An analysis of CMIP5 simulations, *Geophys. Res. Lett.*, *40*, 4018–4024, doi:10.1002/grl.50730.

1. Introduction

[2] Changes in the hydrological cycle are expected to scale with temperature changes. Recent observations, as well as model simulations of the 20th century and the response to anthropogenic increases in CO_2, have shown that precipitation increases in a warming world [*Meehl et al.*, 2007]. The water vapor holding capacity of the lower troposphere increases by ~7% per degree of warming following the Clausius-Clapeyron relationship, which is well approximated by

$$e_s = 0.6108e^{\frac{aT}{b+T}} \tag{1}$$

where e_s is the saturation vapor pressure (kPa), T is air temperature (°C), $a = 17.27$, and $b = 237.3$°C. The observed and simulated changes in precipitation, however, are consistently smaller than the changes in the saturation vapor pressure [*Allan and Soden*, 2007, 2008; *Adler et al.*, 2008; *DiNezio et al.*, 2011]. The difference between the two reflects energetic constraints on evaporation [*Allan*, 2009; *Allen and Ingram*, 2002; *Previdi*, 2010; *Richter and Xie*, 2008]. Equilibrium evaporation, which is the theoretical rate of evaporation (including transpiration) from a large, uniform, wet or well-watered surface, is given by

$$\lambda E_q = R_n \frac{\mathrm{d}e_s/\mathrm{d}T}{\mathrm{d}e_s/\mathrm{d}T + \gamma} \tag{2}$$

where λ is the latent heat of vaporization of water ($\approx 2.45\ \mathrm{MJ\ kg^{-1}}$), R_n is net radiation, and γ is the psychrometer constant ($\approx 0.067\ \mathrm{kPa\ K^{-1}}$ at sea level). The maximum evaporative fraction (the fraction of R_n that can be used for evaporation under equilibrium conditions) increases less steeply than the saturation vapor pressure, ~1%–4% per degree for temperatures in the range of 0°C–30°C (Figure 1). Equation (2) emphasizes the surface energy-balance constraint on evaporation. In contrast, vapor pressure deficit (a key predictor of evaporation in standard bulk formulae [e.g., *Richter and Xie*, 2008]) can be regarded as an outcome of rather than a constraint on evaporation [*Raupach*, 2000]. Indeed, *Richter and Xie* [2008] showed how key boundary layer properties influencing evaporation can change in response to large-scale changes in the surface energy balance. Water availability can place an additional constraint on evaporation from the land surface and hence further mute the increase of continental precipitation as temperature increases [*Trenberth and Shea*, 2005].

[3] Analyses of recent changes in tropical rainfall have shown that precipitation has increased markedly in wet regions and has decreased in subtropical dry regions [*Adler et al.*, 2008; *Allan and Soden*, 2007; *Wentz et al.*, 2007; *Zhang et al.*, 2007; *Allan et al.*, 2010]. This is also a feature of seasonal climates, with summer (monsoon) precipitation increasing more than winter (dry season) precipitation [*Giorgi and Bi*, 2005; *Chou et al.*, 2013]. This phenomenon has been referred to as "the rich get richer" syndrome [*Trenberth*, 2011] and can be explained either as a result of increasing the amount of atmospheric water vapor [*Held and Soden*, 2006] or from diversion of moisture into regions of atmospheric convergence associated with changes in atmospheric circulation [*DiNezio et al.*, 2011]. *Trenberth and Shea* [2005] suggested that a similar syndrome is also characteristic of extratropical regions, which is expected since these are regions of net moisture import from lower latitudes. Model simulations of the 20th and 21st centuries from the last round of the Coupled Model Intercomparison Project (CMIP3) show similar tendencies, with wetting in convergence regions and drying in the subtropics associated

Additional supporting information may be found in the online version of this article.

[1]Department of Biological Sciences, Macquarie University, North Ryde, New South Wales, Australia.
[2]Department of Geography and Environmental Sciences, School of Human and Environmental Sciences, Reading University, Reading, UK.
[3]Department of Geography, University of Oregon, Eugene, Oregon, USA.
[4]AXA Chair of Biosphere and Climate Impacts, Department of Life Sciences and Grantham Institute for Climate Change, Imperial College, Ascot, UK.

Corresponding author: G. Li, Department of Biological Sciences, Macquarie University, North Ryde, NSW 2109, Australia. (guangqi.li@students.mq.edu.au)

0094-8276/13/10.1002/grl.50730

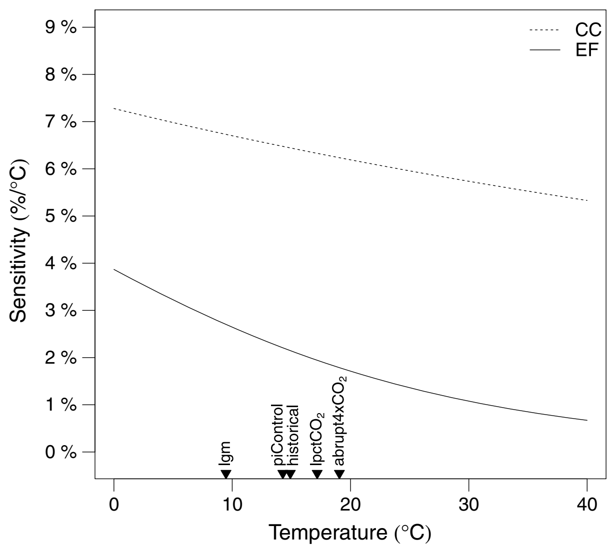

Figure 1. Theoretical limits on the rate of increase of precipitation with temperature, according to alternative hypotheses: (a) following the temperature dependence of the saturated vapor pressure of water, according to the Clausius-Clapeyron relationship (dotted line, CC); (b) following the temperature dependence of the fraction of net radiation that can be used for evaporation under equilibrium conditions (solid line, EF). The global ensemble mean temperature for each of the experiments is shown in order to place the simulated changes in context.

with a strengthening of the Walker circulation [*DiNezio et al*., 2011]. However, the response of the tropical circulation is influenced by multiple processes operating on different time scales (e.g., water vapor [*Bony et al*., 2013]), and the response of precipitation is weaker than that shown by the observational record and differs among different models [*Allan and Soden*, 2008].

[4] The observational record is short, and the strength of the precipitation response to temperature has been controversial [*Wentz et al*., 2007; *Adler et al*., 2008; *Gu et al*., 2007; *Huffman et al*., 2009; *Trenberth*, 2011]. Thus, it is still unclear whether the discrepancy between CMIP3 model results and observations is significant. Recent analyses [*Izumi et al*., 2013] have shown that the simulated large-scale patterns of temperature changes at the Last Glacial Maximum (LGM) are remarkably similar (though of opposite sign) to those shown in raised CO_2 experiments. These signals include changes of comparable magnitude in the land-sea temperature contrast, in the magnitude of high-latitude amplification of temperature changes, and changes in seasonality in response to year-round forcing, and the simulated patterns are consistent with those in paleoclimatic or instrumental observations. Thus, the LGM experiments provide an opportunity to examine precipitation scaling with temperature and the regional patterns of precipitation changes and to determine whether these are consistent with paleo-observations.

[5] Here we analyze outputs from six models that have run both LGM and raised CO_2 experiments in CMIP5. We evaluate whether the raised CO_2 experiments show similar changes in precipitation to the earlier CMIP3 experiments and then examine whether consistent changes are also present in the cold-climate state of the LGM. The LGM is an equilibrium experiment comparable to the CMIP5 4xCO_2 experiment, but we also use the CMIP5 1% CO_2 per year transient experiment in our analyses. Finally, we examine the consistency between simulated and observed changes in precipitation scaling at the LGM and during the historic period to determine whether simulated changes in precipitation are realistic.

2. Methods

[6] Six CMIP5 models (IPSL-CM5A-LR, MPI-ESM-P, MIROC-ESM, CCSM4, MRI-CGCM3, and GISS-E2-R) have performed both the LGM and raised CO_2 experiments. In our analyses, we use five simulations. Following the CMIP5 naming conventions, these are the Last Glacial Maximum (*lgm*), a preindustrial control simulation (*piControl*), a 20th century simulation (*historical*), a transient 1% per year increase in CO_2 over the simulation (*1pctCO$_2$*), and an abrupt change to 4xCO_2 (*abrupt4xCO$_2$*). *lgm*, *piControl*, and *abrupt4xCO$_2$* are equilibrium experiments, and *historical* and *1pctCO$_2$* are transient experiments. The boundary conditions for each experiment are described in *Taylor et al*. [2012]. The *lgm* experiment represents a cold-climate state, in response to low greenhouse gas concentrations and expanded Northern Hemisphere ice sheets. The *1pctCO$_2$* and *abrupt4xCO$_2$* experiments represent warm-climate states, in response to increased greenhouse gas concentrations. The CO_2 concentration at the end of *1pctCO$_2$* is similar to the CO_2 concentration used in the *abrupt4xCO$_2$* experiment. To provide an alternative realization of a warm-climate state, we therefore sampled the middle part of the *1pctCO$_2$* experiment (model years 86–115) when the CO_2 level was approximately 750 ppm. The total forcing in the *lgm* and *4xCO$_2$* experiments is similar but, although greenhouse gases are the dominant contributor to the tropical forcing at the *lgm* experiment, they contribute only about half (2.85 Wm^{-2}) of the total global forcing [*Braconnot et al*., 2012].

[7] To compare the results from different models, with different spatial resolutions, the outputs of each model were regridded onto a common 2° × 2° grid. Land grid-cells were defined as those 2° × 2° cells with a land fraction of >40%. The near-surface air temperature (tas) was used over the land and sea ice–covered sea surface (sic ≥ 40%), and the sea surface temperature (tos) was used over the ocean (sic < 40%). (We use tos for ocean temperatures to facilitate comparisons with historical and paleoreconstructions of sea-surface temperatures; differences in tos and tas in ice-free areas are negligible.) The changes in precipitation and temperature for each experiment and model are expressed as anomalies from that model's *piControl* (experiment minus control), except in the case of the *historical* simulation, where the anomaly is calculated as the difference between the first and last 27 years of the simulation. We adopted this approach because the temperature at the beginning of the *historical* run is different from the corresponding PI simulation for most of the models (CCSM4, GISS-E2-R, IPSL-CM5A-LR, and MIROC-ESM); the 27 year interval is the length of the baseline period used for the calculation of anomalies in the HadCRUT4 data set. Area-averaged values are calculated for the globe, the tropics (here defined as 30°N–30°S) and the extratropics (>30°N and >30°S). We analyzed the seasonal climate changes in terms of changes in the wettest and driest month ((mean precipitation of the wettest month (MPWE) and mean precipitation of the driest month (MPDR)). The delimitation of wet and dry regions was made using precipitation deciles of the

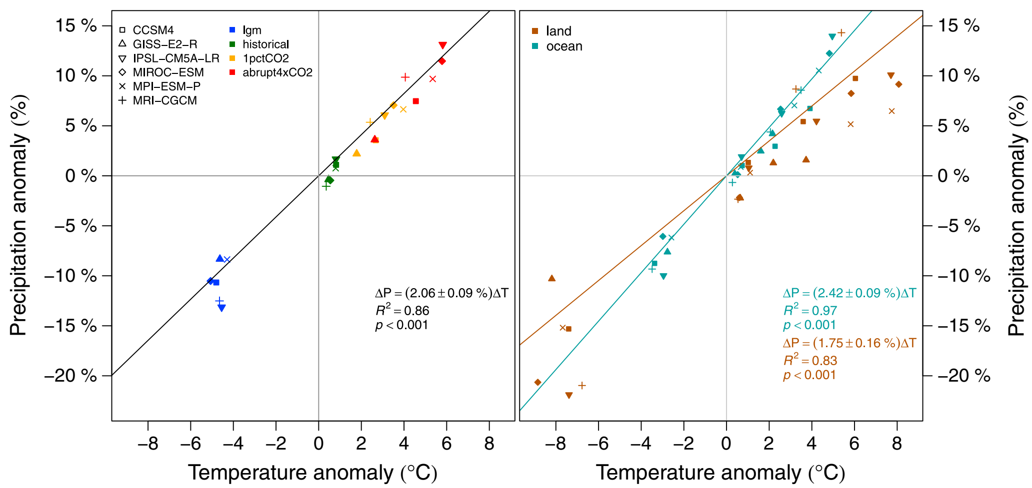

Figure 2. The change in precipitation (%) as a function of the change in global temperature (°C) as simulated by each of the six CMIP5 models (IPSL-CM5A-LR, MPI-ESM-P, MIROC-ESM, CCSM4, MRI-CGCM3, and GISS-E2-R) at the Last Glacial Maximum (LGM), from the historical run (average for period 1979–2005 CE), the 1% CO_2 run (*1pctCO₂*, average for model years 86–115), and the *4xCO₂* run. The left-hand plot shows the global relationship, while the right-hand plots shows the change in global precipitation (%) over (red) land and (blue) ocean as a function of the change in global land and ocean temperature (°C).

piControl for each model in order to capture the most extreme states (although similar results are obtained using, e.g., the upper and lower quartiles of precipitation). This results in different regions being defined as wet or dry in each model.

[8] We evaluate the realism of the *lgm* and *historical* simulations using paleoclimate reconstructions and historical observations over the land. (There are no reconstructions of precipitation over the ocean.) We use a data set of quantitative climate reconstructions for the LGM from S. P. Harrison et al. (Climate model benchmarking with glacial and mid-Holocene climates, submitted to *Climate Dynamics*, 2013). This data set provides reconstructions (including uncertainties) of several climate variables; here we use mean annual temperature over the land and ocean and mean annual precipitation over the land. The historical data are derived from two data sets: temperature data are from the HadCRUT4 combined land and ocean temperature data set [*Morice et al.*, 2012], which covers the period from 1850 to 2009; precipitation data are from the GHCN (Global Historical Climatology Network, Version 2) product, which provides land precipitation data and covers the interval from 1900 to 2010 [*Peterson and Vose*, 1997]. The earliest part of the record is based on very few actual observations; the observed historical change is therefore taken as the difference between the mean for 1979–2005 and the mean for 1941–1970, and the simulated climate is the difference between the same years in the simulations.

3. Results: Simulated Changes

[9] The ensemble averages of the six models (see Figure S1 in the supporting information) illustrate the large changes in temperature and precipitation characteristic of the cold- and warm-climate states. The *lgm* simulations show changes of comparable magnitude (though opposite sign) to the *4xCO₂* simulations, consistent with the fact that the overall forcing is of comparable magnitude [*Braconnot et al.*, 2012], and *historical* and *1pctCO₂* show changes intermediate in magnitude. There are consistent patterns in the large-scale temperature response in warm- and cold-climate states [*Izumi et al.*, 2013]: the land warms/cools more than the oceans, and the high latitudes warm/cool more than the tropics. *Izumi et al.* [2013] also showed that there is a different seasonal response to year-round climate forcing in both warm and cold climates. These large-scale temperature patterns are broadly reflected in the changes in precipitation (Figure S1). In general, there are bigger changes in precipitation over the land than over the ocean in both warm- and cold-climate states. Changes in precipitation in the high latitudes (north of approximately 50°N) are larger than those in the midlatitudes (30°N–50°N), although the response of precipitation in the tropics does not scale straightforwardly with temperature.

[10] There is a strong relationship between changes in global temperature and precipitation, with increased precipitation in a warm climate and decreased precipitation in a cold-climate state (Figure 2). The estimate of the scaling across all the climate states and all models indicates a $2.06\% \pm 0.09\%$ change per degree (Figure 2); estimates based on individual models across the climate states vary between 1.63% and 2.51% per degree. The range of values (Table S1) obtained for the *lgm* experiment (1.80%–2.89%) is similar to that obtained for the *4xCO₂* experiment (1.37%–2.43%). The values for an individual model are always larger in the *lgm* experiment than in the *4xCO₂* experiment, however, consistent with the fact that the energetic limitation on evaporation is smaller in the colder state (Figure 1). The values from the *1pctCO₂* experiment are not consistently larger than those from the *4xCO₂* experiment, but the differences in scaling between the two experiments are small.

[11] The *historical* simulation is the only experiment to include volcanic and solar forcing and changes in aerosols and land use. The simulated changes in temperature over the historic period are small (<1°C), as is the magnitude of the forcing (relative to the *lgm* or *4xCO₂* simulations), though consistent with the magnitude of changes shown by the HadCRUT4 data (Figure S2). The results obtained for the *historical* simulations are anomalous: while some models show an increase in precipitation over the course of the simulation, three models (GISS-E2-R, MIROC-ESM, and

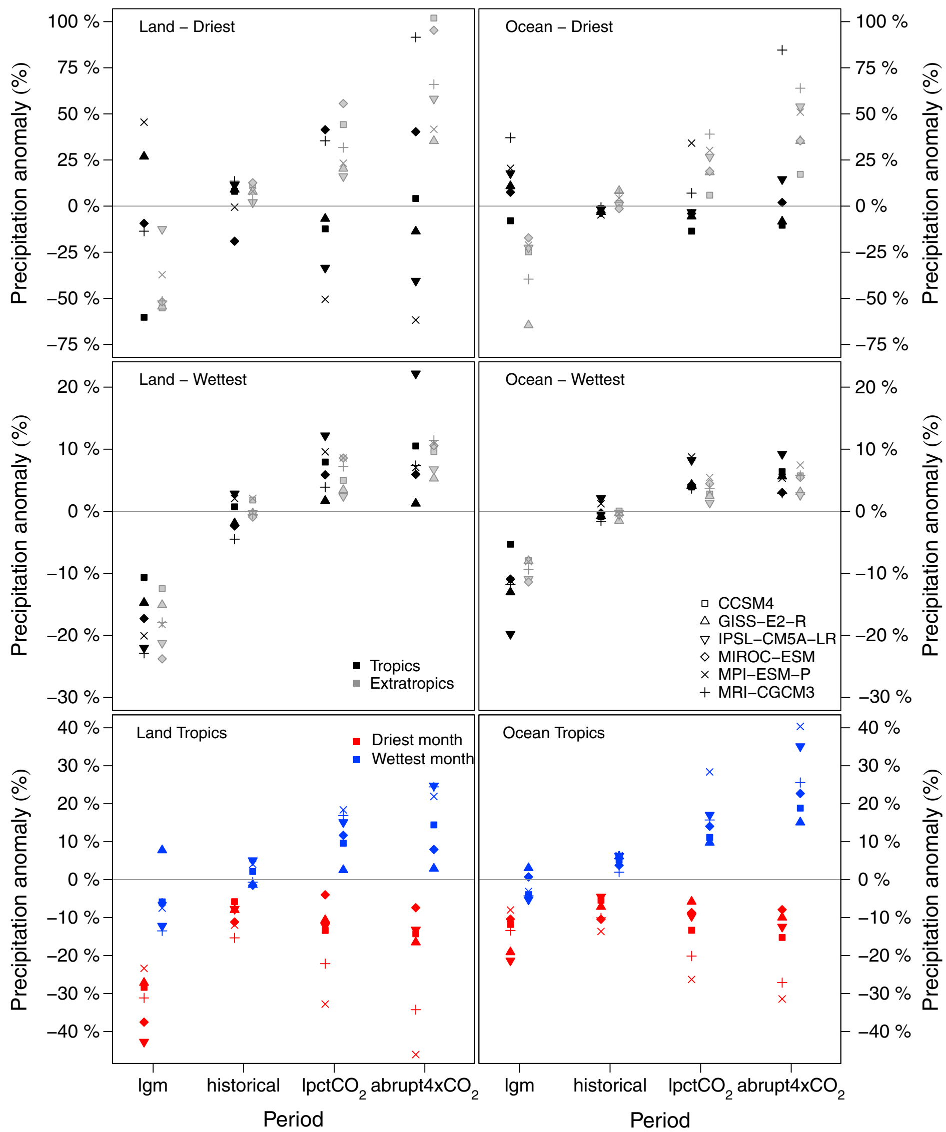

Figure 3. Simulated changes in precipitation (%) in the wettest and driest areas of the tropical (30°N–30°S) and extratropical (>30°N and >30°S) land and ocean. The wettest and driest areas are defined separately for each individual model as those grid cells that fall in the top and bottom deciles of precipitation in the control simulation (*piControl*). Simulated changes in tropical precipitation (%) during the wettest month (MPWE) and the driest month (MPDR) are shown in the bottom panels for comparison.

MRI-CGCM3) show a negative relationship between temperature and precipitation.

[12] To quantify the impact of water availability as a constraint in the *lgm* and raised CO_2 experiments, we estimated the precipitation scaling over the land and ocean separately. The estimate of the scaling across all climate states and all models (Figure 2) indicates a $2.42 \pm 0.09\%$ change per degree over the ocean and a $1.75 \pm 0.16\%$ change over the land. This finding suggests that the change in global precipitation with temperature is slightly reduced because of the additional constraint of water supply on evaporation over land areas. Estimates of the relationship between temperature and precipitation obtained from individual models and experiments generally show that the scaling over the ocean is greater than that over the land (Table S2). Thus, the values obtained for the model ensemble mean for ocean and land, respectively, are 2.64% and 2.28% for the *lgm* experiment, 2.04% and 1.39% for the *1pctCO2* experiment, and 2.32% and 1.33% for the *4xCO$_2$* experiment. Model responses over the ocean are more consistent than those over the land (Figure 2). The variability over the land probably reflects larger differences in treatment of the land among the different models (e.g., number of vegetation types, treatment of soil moisture, effective rooting depth, and inclusion of carbon cycle).

[13] The role of water limitation can also be examined by comparing the scaling over the tropical and extratropical land areas, with the expectation that water supply constraints might be less prominent in extratropical regions. In warm-climate states, the scaling of precipitation with temperature over the extratropical land (mean value, *1pctCO$_2$*: 2.61%/°C and *4xCO$_2$*: 2.77%/°C) is indeed greater than over tropical land areas (mean value, *1pctCO$_2$*: 1.00%/°C and *4xCO$_2$*: 0.72%/°C). This is also generally the case for individual

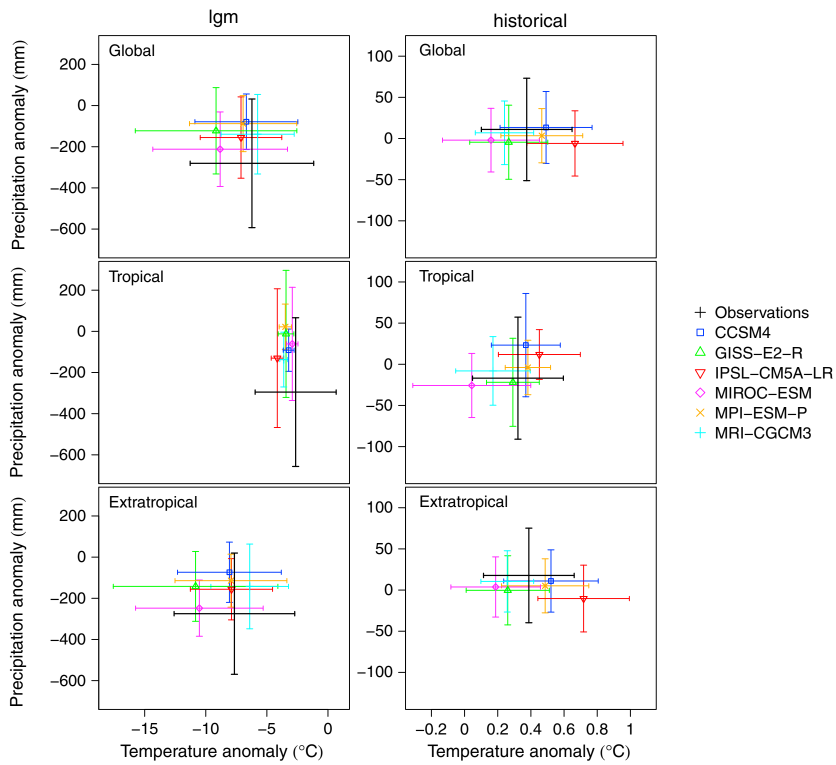

Figure 4. Comparison between climate reconstructions and model simulations over the land. The comparison is based on the model grid cells where observations of both temperature and precipitation are available. The bars show the standard deviation of the spatial values for both observations and model simulations. The historical observations are differences between the 1979–2005 and 1941–1970 long-term means from the GHCN precipitation data set [*Peterson and Vose*, 1997] and the HadCRUT4 temperature data set [*Morice et al.*, 2012]. The paleoclimate reconstructions are from Harrison et al. (submitted manuscript, 2013).

models (Table S2). However, the scaling between temperature and precipitation in the *lgm* experiment is greater over tropical (3.67%/°C) than extratropical (2.87%/°C) land areas (Table S2).

[14] Tropical areas that are wet in the preindustrial period, as defined by the top decile of precipitation, get wetter in warm-climate states and drier in cold-climate states (Figure 3). This is true for both land and ocean regions. The behavior of dry tropical regions, as defined by the lowest decile of precipitation in the preindustrial control state, is less coherent. Half of the models show these regions becoming wetter in the $4xCO_2$ simulation both over the land and over the ocean. At the *lgm* experiment, most of the models show these regions of the ocean getting wetter (five out of six models), as expected, but the models show both wetting (three models) and drying (three models) over the land. Thus, the models show a robust response of wet environments to temperature changes, but the nature of the precipitation changes in dry regions, particularly dry land regions, is model dependent. These findings are not sensitive to the definition of wet and dry regions: similar numbers of models show wetting/drying, for example, when the regions are defined using the top/bottom quartile of preindustrial precipitation. Extratropical areas that are wet in the preindustrial period get wetter in warm climates and drier in cold climates (Figure 3). However, this is also true for extratropical areas that are dry in the preindustrial period. Thus, the "rich get richer" syndrome is a characteristic of tropical climates but has no parallel in the extratropics.

[15] Precipitation is highly seasonal over most of the tropics, with summer (monsoon) rain and drier conditions in winter. Summer precipitation (as indexed by MPWE) increases while winter precipitation (as indexed by MPDR) decreases over both the land and the ocean in warm-climate states (Figure 3), leading to a significant increase in precipitation seasonality. In a cold world (Figure 3), there are precipitation decreases in both MPDR and MPWE; although the changes are proportionally larger in MPDR, the absolute changes are large in summer, and thus, these changes result in an overall decrease in precipitation seasonality. Thus, the change in tropical precipitation in both warm- and cold-climate states is consistent with the rich get richer syndrome and consistent with the idea [*Chou et al.*, 2007] that changes in precipitation are associated with strengthening (in warm-climate states) and weakening (in cold-climate states) of the monsoons. The Afro-Asian monsoon is weaker in the *lgm* experiments (see also *Braconnot et al.*, 2007), a feature which is also shown by palaeoenvironmental evidence [*Harrison and Bartlein*, 2012].

4. Results: Comparison With Observations

[16] Paleoclimate reconstructions show generally colder and drier conditions over the land at the LGM. The simulated changes in temperature (at grid cells where there are paleoclimate reconstructions) are colder than observed (Figure 4). Nevertheless, the simulated change in precipitation is systematically less than observed, both in the tropics and

extratropics. Thus, the scaling between temperature and precipitation changes in the models appears to be somewhat weaker than observed. However, the comparison for the historical period (Figure 4) does not show a marked discrepancy between the observed and simulated changes in precipitation scaling with temperature. In the tropics, the models showing greater warming over the land than the observations are also wetter, and those that show cooler conditions are drier. In the extratropics, most models show increased temperatures and little or no change in precipitation, whereas the observations show modest increases in both temperature and precipitation. Given the failure to identify a systematic bias in the historical simulations, it seems likely that differences between simulated and observed changes at the LGM are within the range of observational uncertainty.

5. Discussion and Conclusions

[17] Global precipitation increases with warming and decreases with cooling. The relationship, as estimated here from the individual models and simulations, varies between 1.5 and 3% per degree. This range is consistent with previous model-based estimates of precipitation changes during the 20th century [*Held and Soden*, 2006], using future scenarios [*Allen and Ingram*, 2002; *Held and Soden*, 2006], and based on PMIP2 LGM experiments [*Boos*, 2012].

[18] There are consistent patterns in the nature of the scaling of large-scale precipitation changes with temperature in warm- and cold-climate states. Thus, the change in precipitation with temperature is greater over the ocean than over the land in both warm and cold climates. Similarly, over land areas, the change in precipitation per degree temperature change is larger in the extratropics than the tropics. Changes in tropical precipitation are greatest in areas that are currently wet, resulting in increased precipitation in warm-climate states and decreased precipitation in cold-climate states. The seasonality of precipitation in the tropics also changes in a consistent way, with increased seasonality in warm-climate states and decreased seasonality in cold-climate states.

[19] At global and regional scales, the scaling of precipitation change with temperature is consistently much less than the 7% per degree change in atmospheric water vapor predicted by the Clausius-Clapeyron relationship, but consistent with the values expected taking into account energetic constraints on evaporation (~1%–4% per degree for temperatures in the range of 0°C–30°C). The steeper scaling over the ocean compared to the land, and over the extratropical land compared to the generally more arid tropical land, suggests that water limitations reduce modeled precipitation/temperature scaling by about a quarter.

[20] Both the spatial patterns and the scaling relationships are broadly consistent with earlier analyses [see, e.g., *Held and Soden*, 2006; *Liu et al*., 2009; *Previdi*, 2010; *Boos*, 2012]. The response of precipitation in 20th century simulations is generally weaker than that shown by the observational record [*Allan and Soden*, 2008]. The results presented here show that the same applies to the response of precipitation differences between *lgm* and present. However, evaluation using *historical* observations suggests that differences between the observed and simulated precipitation scaling do not exceed the reconstruction uncertainty. Broadly speaking, the evaluations suggest that models are able to capture the large-scale constraints on precipitation scaling in a realistic way.

[21] The inclusion of paleosimulations in the CMIP5 suite of model experiments makes it possible to demonstrate the robustness of simulated behavior across a wider range of climates. More importantly, it offers additional possibilities for model evaluation. Our analyses show that the energetic constraints on evaporation (and water limitation over the land) constrain the simulated changes in precipitation scaling with temperature in a realistic way. While improvements in the availability of paleoclimate reconstructions, and analysis of precipitation scaling over a wider range of paleoclimates, would be useful, these analyses demonstrate the utility of inclusion of paleoclimate simulations as CMIP5 experiments.

[22] **Acknowledgments.** We acknowledge the World Climate Research Programme's Working Group on Coupled Modelling, which is responsible for CMIP, and the climate modeling groups for producing and making available their model output. (For CMIP, the U.S. Department of Energy's Program for Climate Model Diagnosis and Intercomparison provided coordinating support and led the development of the software infrastructure in partnership with the Global Organization for Earth System Science Portals.) The analyses and figures are based on data archived at CMIP5 on 15 August 2012. G.L. is supported by an International Postgraduate Research Scholarship at Macquarie University. This research was supported by the Australian Research Council under grant DP1201100343 (S.P.H.) and by the U.S. National Science Foundation under grant ATM-0602409 (P.J.B. and K.I.).

[23] The Editor thanks two anonymous reviewers for their assistance in evaluating this paper.

References

Adler, R. F., G. Gu, J. J. Wang, G. J. Huffman, S. Curtis, and D. Bolvin (2008), Relationships between global precipitation and surface temperature on interannual and longer timescales (1979–2006), *J. Geophys. Res.*, *113*, D22104, doi:10.1029/2008JD010536.

Allan, R. P. (2009), Examination of relationships between clear-sky longwave radiation and aspects of the atmospheric hydrological cycle in climate models, reanalyses, and observations, *J. Clim.*, *22*(11), 3127–3145, doi:10.1175/2008JCLI2616.1.

Allan, R. P., and B. J. Soden (2007), Large discrepancy between observed and simulated precipitation trends in the ascending and descending branches of the tropical circulation, *Geophys. Res. Lett.*, *34*, L18705, doi:10.1029/2007GL031460.

Allan, R. P., and B. J. Soden (2008), Atmospheric warming and the amplification of precipitation extremes, *Science*, *321*(5895), 1481–1484, doi:10.1126/science.1160787.

Allan, R. P., B. J. Soden, V. O. John, W. Ingram, and P. Good (2010), Current changes in tropical precipitation, *Environ. Res. Lett.*, *5*(2), 025205, doi:10.1088/1748-9326/5/2/025205.

Allen, M. R., and W. J. Ingram (2002), Constraints on future changes in climate and the hydrologic cycle, *Nature*, *419*(6903), 224–232, doi:10.1038/nature01092.

Bony, S., G. Bellon, D. Klocke, S. Sherwood, S. Fermepin, and S. Denvil (2013), Robust direct effect of carbon dioxide on tropical circulation and regional precipitation, *Nat. Geosci.*, doi:10.1038/NGEO1799.

Boos, W. R. (2012), Thermodynamic scaling of the hydrological cycle of the last glacial maximum, *J. Clim.*, *25*(3), 992–1006, doi:10.1175/JCLI-D-11-00010.1.

Braconnot, P., et al. (2007), Results of PMIP2 coupled simulations of the mid-Holocene and Last Glacial Maximum, Part 1: Experiments and large-scale features, *Clim. Past*, *3*, 261–277.

Braconnot, P., S. P. Harrison, M. Kageyama, P. J. Bartlein, V. Masson-Delmotte, A. Abe-Ouchi, B. Otto-Bliesner, and Y. Zhao (2012), Evaluation of climate models using paleoclimatic data, *Nat. Clim. Change*, *2*, 417–424, doi:10.1038/nclimate1456.

Chou, C., J.-Y. Tu, P.-H. Tan (2007), Asymmetry of tropical precipitation change under global warming, *Geophys. Res. Lett.*, *34*, L17708, doi:10.1029/2007GL030327.

Chou, C., J. C. H. Chiang, C.-W. Lan, C.-H. Chung, Y.-C. Liao, and C.-J. Lee (2013), Increase in the range between wet and dry season precipitation, *Nat. Geosci.*, doi:10.1038/NGEO1744.

DiNezio, P., A. Clement, G. Vecchi, B. Soden, A. Broccoli, B. Otto-Bliesner, and P. Braconnot (2011), The response of the Walker circulation to Last Glacial Maximum forcing: Implications for detection in proxies, *Paleoceanography*, *26*, PA3217, doi:10.1029/2010PA002083.

Giorgi, F., and X. Bi (2005), Updated regional precipitation and temperature changes for the 21st century from ensembles of recent

AOGCM simulations, *Geophys. Res. Lett.*, *32*, L21715, doi:10.1029/2005GL024288.

Gu, G., R. F. Adler, G. J. Huffman, and S. Curtis (2007), Tropical rainfall variability on interannual-to-interdecadal and longer time scales derived from the GPCP monthly product, *J. Clim.*, *20*(15), 4033–4046, doi:10.1175/JCLI4227.1.

Harrison, S. P., and P. J. Bartlein (2012), Records from the past, lessons for the future: what the palaeo-record implies about mechanisms of global change, in *The Future of the World's Climates*, edited by A. Henderson-Sellers, and K. McGuffie, pp. 403–436, Elsevier, Oxford, UK.

Held, I. M., and B. J. Soden (2006), Robust responses of the hydrological cycle to global warming, *J. Clim.*, *19*(21), 5686–5699, doi:10.1175/JCLI3990.1.

Huffman, G. J., R. F. Adler, D. T. Bolvin, and G. Gu (2009), Improving the global precipitation record: GPCP version 2.1, *Geophys. Res. Lett.*, *36*, L17808, doi:10.1029/2009GL040000.

Izumi, K., P. J. Bartlein, and S. P. Harrison (2013), Consistent behaviour of the climate system in response to past and future forcing, *Geophys. Res. Lett.*, *40*, 1817–1823, doi:10.1002/grl.50350.

Liu, S. C., C. Fu, C.-J. Shiu, J.-P. Chen, and F. Wu (2009), Temperature dependence of global precipitation extremes, *Geophys. Res. Lett.*, *36*, L17702, doi:10.1029/2009GL040218.

Meehl, G. A., et al. (2007), Global climate projections, in *Climate Change 2007: The Physical Science Basis, Contribution of Working Group I to the Fourth Assessment Report of the Intergovernmental Panel on Climate Change*, edited by S. Solomon et al., pp. 749–845, Cambridge Univ. Press, Cambridge, United Kingdom and New York, NY, USA.

Morice, C. P., J. J. Kennedy, N. A. Rayner, and P. D. Jones (2012), Quantifying uncertainties in global and regional temperature change using an ensemble of observational estimates: The HadCRUT4 dataset, *J. Geophys. Res.*, *117*, D08101, doi:10.1029/2011JD017187.

Peterson, T. C., and R. S. Vose (1997), An overview of the Global Historical Climatology Network temperature database, *Bull. Am. Meteorol. Soc.*, *78*(12), 2837–2849, doi:10.1175/1520-0477(1997)078<2837:AOOTGH>2.0.CO;2.

Previdi, M. (2010), Radiative feedbacks on global precipitation, *Environ. Res. Lett.*, *5*, 025211, doi:10.1088/1748-9326/5/2/025211.

Raupach, M. (2000), Equilibrium evaporation and the convective boundary later, *Boundary Layer Meteorol.*, *96*, 107–142.

Richter, I., and S. P. Xie (2008), Muted precipitation increase in global warming simulations: A surface evaporation perspective, *J. Geophys. Res.*, *113*, D24118, doi:10.1029/2008JD010561.

Taylor, K. E., R. J. Stouffer, and G. A. Meehl (2012), An overview of CMIP5 and the experiment design, *Bull. Am. Meteorol. Soc.*, *93*(4), 485, doi:10.1175/BAMS-D-11-00094.1.

Trenberth, K. E. (2011), Changes in precipitation with climate change, *Clim. Res.*, *47*(1), 123, doi:10.3354/cr00953.

Trenberth, K. E., and D. J. Shea (2005), Relationships between precipitation and surface temperature, *Geophys. Res. Lett.*, *32*, L14703, doi:10.1029/2005GL022760.

Wentz, F. J., L. Ricciardulli, K. Hilburn, and C. Mears (2007), How much more rain will global warming bring?, *Science*, *317*(5835), 233–235, doi:10.1126/science.1140746.

Zhang, X., F. W. Zwiers, G. C. Hegerl, F. H. Lambert, N. P. Gillett, S. Solomon, P. A. Stott, and T. Nozawa (2007), Detection of human influence on twentieth-century precipitation trends, *Nature*, *448*(7152), 461–465, doi:10.1038/nature06025.